Hole-Doped Cuprate Panorama and the Second Neighbor Hopping

P. Goswami*
Deshbandhu College, University of Delhi, Kalkaji, New Delhi-110019, India

(Received August 6, 2012; in final form March 13, 2013)

We consider the coexistent id-density wave order, at the antiferromagnetic wave vector $\boldsymbol{Q} = (\pi, \pi)$, representing the pseudo-gap state, and d-wave superconductivity, driven by an assumed attractive interaction, within the BCS framework for the two-dimensional fermion system on a square lattice starting with a mean-field Hamiltonian involving the singlet id-density wave and the d-wave superconductivity pairings. The second-neighbor hopping, which is known to be important for cuprates and frustrates the kinetic energy of electrons, leads to the Fermi surface sheets being not connected by $\boldsymbol{Q}$. The signature of the particle–hole asymmetry in the single-particle excitation spectrum of the pure id-density wave state is reflected in the coexisting id-density wave and d-wave superconductivity states, though the latter is characterized by the Bogoliubov quasi-particle bands — a characteristic feature of superconducting state. Quite significantly, we find that the coexistence is possible due to the non-nesting property.

DOI: 10.12693/APhysPolA.124.90
PACS: 74.72.Gh, 74.20.−z

1. Introduction

There are divergent views regarding the origin of the pseudo-gap (PG) phase and its relation with d-wave superconductivity (DSC). The interpretations run from expositions where the PG is regarded as a superconducting precursor state involving incoherent electron–electron pairings above T_c [1, 2] with particle–hole symmetry of the SC state preserved to others where the PG, distinct from SC, corresponds to an ordered state with particle–hole asymmetry and both the phases compete [3, 4]. In the former, for the underdoped regime, the pre-formed pairs appear at relatively high temperatures $T^* \approx 200$ K compared to $T_c \approx 100$ K and one views T^* as a "crossover" temperature, rather than a sharp phase transition. The origin of these preformed pairs is not fully known. Our view regarding the origin of the PG is, however, centered around the simple paradigm that PG corresponds to id-density wave (DDW) ordering [4] at the antiferromagnetic wave vector $\boldsymbol{Q} = (\pi, \pi)$. Starting with a two-dimensional fermion system on a square lattice described by a mean-field Hamiltonian involving the singlet DDW order ($\mathrm{i}\Delta_{\boldsymbol{k}} = (\mathrm{i}\Delta_0(T)/2)\,(\cos k_x a - \cos k_y a)$) at the wave vector $\boldsymbol{Q} = (\pi, \pi)$, we intend to show that the finger-print of the particle–hole asymmetry (PHA) in the single-particle excitation spectrum of the pure DDW state is reflected in the coexisting DDW and DSC states though the latter is characterized by the Bogoliubov quasi-particle bands — a characteristic feature of SC state. We find that one of the necessary conditions for the coexistence to take place is the "imperfect nesting".

*e-mail: physicsgoswami@gmail.com

2. Theory

In the second-quantized notation, the Hamiltonian to deal with the DDW order at the antiferromagnetic wave vector $\boldsymbol{Q} = (\pi, \pi)$ plus the d-wave superconductivity can be expressed as

$$
\begin{aligned}
H = &\sum_{\boldsymbol{k},\boldsymbol{\sigma}} \varepsilon_{\boldsymbol{k}} d^{\dagger}_{\boldsymbol{k},\boldsymbol{\sigma}} d_{\boldsymbol{k},\boldsymbol{\sigma}} + \sum_{\boldsymbol{k},\boldsymbol{\sigma}} \varepsilon_{\boldsymbol{k}+\boldsymbol{Q}} d^{\dagger}_{\boldsymbol{k}+\boldsymbol{Q},\boldsymbol{\sigma}} d_{\boldsymbol{k}+\boldsymbol{Q},\boldsymbol{\sigma}} \\
&+ \sum_{\boldsymbol{k},\boldsymbol{\sigma}} D_{\boldsymbol{k}} d^{\dagger}_{\boldsymbol{k},\boldsymbol{\sigma}} d_{\boldsymbol{k}+\boldsymbol{Q},\boldsymbol{\sigma}} + \sum_{\boldsymbol{k},\boldsymbol{\sigma}} D^{\dagger}_{\boldsymbol{k}} d^{\dagger}_{\boldsymbol{k}+\boldsymbol{Q},\boldsymbol{\sigma}} d_{\boldsymbol{k},\boldsymbol{\sigma}} \\
&+ \sum_{\boldsymbol{k},\boldsymbol{\sigma}} \Delta^{\dagger(\mathrm{SC})}_{\boldsymbol{k}} d_{-\boldsymbol{k},-\boldsymbol{\sigma}} d_{\boldsymbol{k},\boldsymbol{\sigma}} + \sum_{\boldsymbol{k},\boldsymbol{\sigma}} \Delta^{(\mathrm{SC})}_{\boldsymbol{k}} d^{\dagger}_{\boldsymbol{k},\boldsymbol{\sigma}} d^{\dagger}_{-\boldsymbol{k},\boldsymbol{\sigma}} \\
&- \mu \sum_{\boldsymbol{k},\boldsymbol{\sigma}} (d^{\dagger}_{\boldsymbol{k},\boldsymbol{\sigma}} d_{\boldsymbol{k},\boldsymbol{\sigma}} + d^{\dagger}_{\boldsymbol{k}+\boldsymbol{Q},\boldsymbol{\sigma}}, d_{\boldsymbol{k}+\boldsymbol{Q},\boldsymbol{\sigma}}), \qquad (1)
\end{aligned}
$$

where $D_{\boldsymbol{k}} = (\mathrm{i}\Delta_{\boldsymbol{k}}) \equiv -\sum_{-\boldsymbol{k}',\boldsymbol{\sigma}} U(\boldsymbol{k},\boldsymbol{k}')\langle d^{\dagger}_{\boldsymbol{k}'+\boldsymbol{Q},\boldsymbol{\sigma}} d_{-\boldsymbol{k}',\boldsymbol{\sigma}}\rangle$. The quantity μ is the chemical potential of the fermion number. The imaginary d-wave order parameter $D_{\boldsymbol{k}}$ describing the PG state breaks the time-reversal symmetry of the normal state. In (1), $d_{\boldsymbol{k},\boldsymbol{\sigma}}$, with $\boldsymbol{\sigma} = \pm 1$, corresponds to the fermion annihilation operator for the single-particle state $(\boldsymbol{k},\boldsymbol{\sigma})$. The DSC gap function $\Delta^{\dagger(\mathrm{SC})}_{\boldsymbol{k}} \equiv \sum_{-\boldsymbol{k}',\boldsymbol{\sigma}} V(\boldsymbol{k},\boldsymbol{k}')\langle d^{\dagger}_{-\boldsymbol{k}',\boldsymbol{\sigma}} d^{\dagger}_{-\boldsymbol{k}',-\boldsymbol{\sigma}}\rangle = -\Delta^{\dagger(\mathrm{SC})}_{\boldsymbol{k}+\boldsymbol{Q}}$. The conical brackets stand for the thermal average calculated with the Hamiltonian in (1). This ensures the self-consistency. The interaction $U(\boldsymbol{k},\boldsymbol{k}')$, with Coulombic origin [4], is of the form $U(\boldsymbol{k},\boldsymbol{k}') = |U_1|(\cos k_x a - \cos k_y a)(\cos k'_x a - \cos k'_y a)$. Upon substituting this in $D_{\boldsymbol{k}} = -\sum_{-\boldsymbol{k}',\boldsymbol{\sigma}} U(\boldsymbol{k},\boldsymbol{k}')\langle d^{\dagger}_{\boldsymbol{k}'+\boldsymbol{Q},\boldsymbol{\sigma}} d_{\boldsymbol{k}',\boldsymbol{\sigma}}\rangle$, we obtain the DDW gap equation. The DSC order parameter $\Delta^{(\mathrm{SC})}_{k}$, on the other hand, requires an appropriate attractive interactions $V(\boldsymbol{k},\boldsymbol{k}') = -|V_1|(\cos k_x a - \cos k_y a)(\cos k'_x a - \cos k'_y a)$, where V_1 is the coupling strength, and the corresponding

gap equation is obtained in the similar manner. The time-reversal invariance of the normal state requires that the dispersion $\varepsilon_{\boldsymbol{k}} = \varepsilon_{-\boldsymbol{k}}$. We assume a tight-binding non-nested dispersion of the form

$$\varepsilon_{\boldsymbol{k}} = -2t_1\,(\cos k_x a + \cos k_y a) + 4t_2 \cos k_x a \cos k_y a - 2t_3(\cos 2k_x a + \cos 2k_y a) + 4t_2, \quad (2)$$

where, for the hole-doped materials, $t_2 > 0$ (for the electron-doped materials $t_2 < 0$), and, in all cases, $t_2 < t_1/2$. For example, typical values are $t_1 \approx 0.20$ eV, $t_2/t_1 \approx 0.40$, and $t_3/t_1 \approx 0.01$. Upon ignoring the third neighbor hopping term above, we find that the dispersion typically has two in-equivalent saddle point van Hove singularities (vHS) at $(\pi, 0)$ and $(0, \pi)$ in the first Brillouin zone [5]. Upon assuming that for fillings such that the Fermi curve lies close to the singularities, the majority of states participating in the pairing formation alluded to above will come from regions in the vicinity of these saddle points. This is the strategy we have adopted, so that even arbitrarily weak interactions can produce large effects in the physical quantities of interest via the density-of-states (DOS) or the single--particle spectral function $A(\boldsymbol{k}, \omega)$. For the pure DDW case, the spectral function $A(\boldsymbol{k}, \omega)$ is given approximately by a sum of δ functions at the quasi-particle energies: $A(\boldsymbol{k}, \omega) = 2\pi[u^2_{\boldsymbol{k}}\delta(\omega - \varepsilon^{(U)}_{\boldsymbol{k}}) + v^2_{\boldsymbol{k}}\delta(\omega - \varepsilon^{(L)}_{\boldsymbol{k}})]$ where the quasi-particle coherence factors $(u^2_{\boldsymbol{k}}, v^2_{\boldsymbol{k}})$ are given by the expressions $u^2_{\boldsymbol{k}} = (1/2)[1 + (\varepsilon^L_{\boldsymbol{k}}/w_{\boldsymbol{k}})]$, $v^2_{\boldsymbol{k}} = (1/2)[1 - (\varepsilon^L_{\boldsymbol{k}}/w_{\boldsymbol{k}})]$. Here $\varepsilon^{(U,L)}_{\boldsymbol{k}} = [\varepsilon^U_k + jw_{\boldsymbol{k}}]$, $\varepsilon^U_{\boldsymbol{k}} = (\xi_{\boldsymbol{k}} + \xi_{\boldsymbol{k}+\boldsymbol{Q}})/2$, $\varepsilon^L_{\boldsymbol{k}} = (\xi_{\boldsymbol{k}} - \xi_{\boldsymbol{k}+\boldsymbol{Q}})/2$, $\xi_{\boldsymbol{k}} = \varepsilon_{\boldsymbol{k}} - \mu$, and $w_{\boldsymbol{k}} = [(\varepsilon^L_{\boldsymbol{k}})^2 + |D_{\boldsymbol{k}}|^2]^{1/2}$. The index j is equal to (± 1) with $j = +1$ corresponding to the upper branch (U) and $j = -1$ to the lower branch (L). These results are the same as those reported by Chakravarty et al. [4]. In particular, if the dispersion is nested (the Fermi surface sheets are connected by $\boldsymbol{Q} = (\pi, \pi)$), we obtain Bogoliubov-like dispersion $\varepsilon^{(U,L)}_{\boldsymbol{k}} = jw_{\boldsymbol{k}}$, and $D^\dagger_{\boldsymbol{k}} = \sum_{\boldsymbol{k'},\boldsymbol{\sigma}} U(\boldsymbol{k}, \boldsymbol{k'})(D^\dagger_{\boldsymbol{k'}}/2w_{\boldsymbol{k'}}) \tanh(\beta w_{\boldsymbol{k'}}/2)$ where $\beta = (k_{\rm B}T)^{-1}$, but the coherence factors $u^2_{\boldsymbol{k}} = 1$ and $v^2_{\boldsymbol{k}} = 0$. This situation manifestly being inadmissible, we consider a imperfectly nested dispersion as in Eq. (2). It also demonstrates plainly that one of necessary conditions for the existence of DDW and the coexistence of DDW and DSC, etc. is the non-nesting property of the normal state dispersion.

3. Results and discussion

It is well known [5] that vHSs lead to a logarithmically diverging DOS. We have plotted the square lattice tight band DOS in the Hubbard model to show this topological feature in Fig. 1. There is logarithmic singularity at the centre and the step-like discontinuities at the band-edges. The particle–hole symmetry arises if the dispersion is nested. We find that even the non-nested dispersion of the form (2) in the presence of DDW ordering is unable to alter the robust divergence feature: the 2D plot of the dimensionless DOS as a function of energy E expressed in units of the nearest neighbor hopping t_1 (in Fig. 1), calculated with Eqs. (1) and (2) in the pseudo-gap phase at the doping level $\approx 10\%$, shows a cusp at $E = 0$. We have rendered DOS dimensionless using the same first neighbor hopping term. However, as regards the symmetry feature, the next-nearest-neighbor hopping (t_2), which is known to be important for cuprates [6] and frustrates the kinetic energy of electrons, leads to the Fermi surface sheets being not connected by $\boldsymbol{Q}$. This manifests itself in the form of PHA in our plot in Fig. 1. We shall show later in Fig. 2 that the signature of this exists in the form of back-bending (or saturation) momentum of the dispersion when the PG and SC phases are coexistent in the under-doped regime (the doping level $\leq 10\%$). However, when the doping level ($\approx 12\%$) is closer to the optimal doping [7], the finger-print appears to be not so prominent possibly due to fact that the doping beyond the optimal level yields normal metals with the Fermi liquid behavior. The signature is an indication of the interplay of the DDW and DSC states.

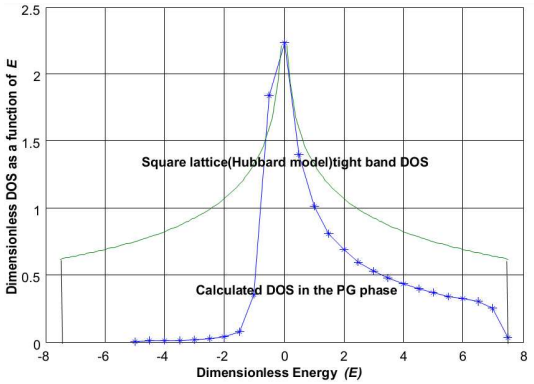

Fig. 1. The 2D plot of the dimensionless spectral function $A(E) = \int_{-\pi}^{+\pi} \mathrm{d}(k_x a)/2\pi \int_{-\pi}^{+\pi} (\mathrm{d}(k_y a)/2\pi A(\boldsymbol{k}, E)t_1$ as a function of energy E, with a cusp at $E = 0$. The numerical values used, in the units of the first neighbor hopping t_1 are $(\mu/t_1) = -0.0189$ (the DDW ordering leads to pinning of the Fermi level close to the vHs), the PG gap amplitude $(\Delta^{(\rm PG)}/t_1) = 0.0871$, and the SC gap amplitude $(\Delta^{(\rm SC)}/t_1) = 0$. The hopping parameters are $(t_2/t_1) = 0.3925$, and $(t_3/t_1) = 0.0005$. The negative energy states by and large correspond to $\boldsymbol{k}$'s close to Γ-point whereas positive energy states are close to $(\pm\pi, \pm\pi)$. We have also plotted the square lattice tight band DOS in the Hubbard model which clearly shows vHS at $E = 0$. The particle–hole symmetry (asymmetry) in the latter (former) is easy to notice.

If the pairing interaction $V(\boldsymbol{k}, \boldsymbol{k'})$ is imagined to be a "probe" applied to the Fermi system in the PG state, then the gap function $\Delta^{(\rm SC)}_{\boldsymbol{k}}$ (where $\Delta^{(\rm SC)}_{\boldsymbol{k}} = \Delta^{\dagger\,(\rm SC)}_{\boldsymbol{k}}$) is perhaps a "response" that the system displays. The structure of the "probe" in momentum space will have tremendous influence on the "response". For example, the usual electron–phonon (e–ph) type pairing interaction leads to a fully gapped state — a "conventional" BCS superconductor. We have assumed here that a combina-

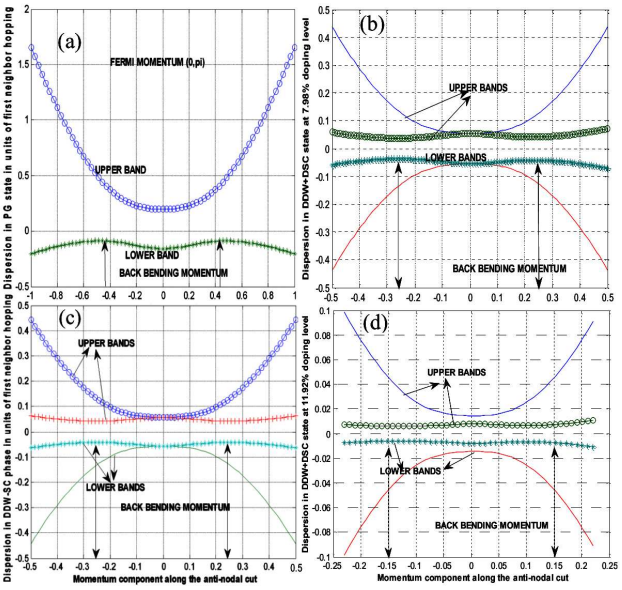

Fig. 2. The plots of the upper and the lower bands in the pure DDW state (a) and in the DDW+DSC state at doping levels 7.98%, 9.94% and 11.92% ((b), (c), and (d)) shown as a function of momentum (k) along the antinodal cut $(-\pi,\pi)$–$(0,\pi)$–(π,π). (a) The back--bending (or saturation) momentum of the dispersion and the Fermi momentum ($k_{\rm F}$) are indicated. The numerical values, in the units of the first neighbor hopping t_1 are $\mu/t_1 = -0.0183$, the PG gap amplitude $\Delta^{(\rm PG)}/t_1 = 0.0610$, and the SC gap amplitude $\Delta^{(\rm SC)}/t_1 = 0$. The hopping parameters are $t_2/t_1 = 0.3925$, and $t_3/t_1 = 0.0005$. (b) There are four quasi--particle bands with two positioned at negative energy and two at positive energy for the Fermi energy taken as zero. The doping level is 7.98% and the temperature $T = 60$ K. The parameter values used are $\mu/t_1 = -0.0017$, the PG gap amplitude $\Delta^{(\rm PG)}/t_1 = 0.023$, and the SC gap amplitude $\Delta^{(\rm SC)}/t_1 = 0.014$. The hopping parameters are $t_2/t_1 = 0.3835$, and $t_3/t_1 = 0.0005$. The orderings lead to pinning of the Fermi level close to, but not precisely at the van Hove singularity. (c) The nearly constant back-bending (or saturation) momentum $(\pm 0.25, \pi)$ of the dispersion as in the previous case is indicated for the doping level 9.94% and the temperature 60 K. The parameter values used are $\mu/t_1 = -0.0018$, the PG gap amplitude $\Delta^{(\rm PG)}/t_1 = 0.024$, and the SC gap amplitude $\Delta^{(\rm SC)}/t_1 = 0.015$. The hopping parameters are $t_2/t_1 = 0.3913$, and $t_3/t_1 = 0.0005$. (d) The less prominent back-bending (or saturation) momentum $(\pm 0.15, \pi)$ of the dispersion is indicated for the doping level 11.92% and the temperature 85.8967 K. The parameter values used are $\mu/t_1 = -0.0054$, the PG gap amplitude $\Delta^{(\rm PG)}/t_1 = 0.0044$, and the SC gap amplitude $\Delta^{(\rm SC)}/t_1 = 0.0032$. The hopping parameters are $t_2/t_1 = 0.3925$, and $t_3/t_1 = 0.0005$. The orderings, as before, lead to pinning of the Fermi level close to, but not precisely at the van Hove singularity.

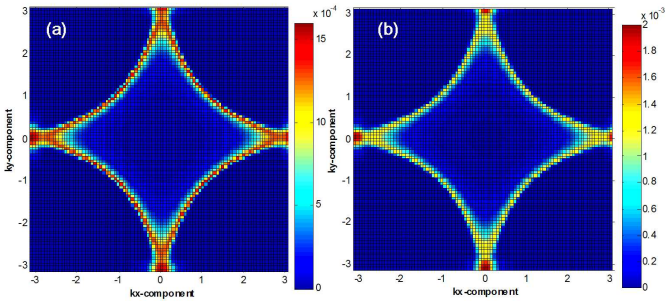

Fig. 3. (a) The contour plot of the momentum dependent carrier density in PG+SC state at 9.94% doping level in the first Brillouin zone. The numerical values, in the units of the first neighbor hopping t_1 are $\mu/t_1 = -0.00183$, the PG gap amplitude $\Delta^{(\rm PG)}/t_1 = 0.0240$, the SC gap amplitude $\Delta^{(\rm SC)}/t_1 = 0.0150$, and the temperature $T = 60$ K. The hopping parameters are $t_2/t_1 = 0.39125$, and $t_3/t_1 = 0.0005$. (b) The contour plot of the momentum dependent carrier density in PG+SC state at 11.92% doping level in the first Brillouin zone. The numerical values, in the units of the first neighbor hopping t_1 are $\mu/t_1 = -0.0054$, the PG gap amplitude $\Delta^{(\rm PG)}/t_1 = 0.0044$, the SC gap amplitude $\Delta^{(\rm SC)}/t_1 = 0.0032$, and the temperature $T = 85.8967$ K. The hopping parameters are $t_2/t_1 = 0.3925$, and $t_3/t_1 = 0.0005$.

tion of electron–electron and/or electron–bosonic mode interactions will lead to a d-wave gap $\Delta^{(\rm SC)}_{\boldsymbol{k}}$. With this assumption, we introduce few thermal averages determined by H, viz. $G_\sigma(\boldsymbol{k},\tau) = -\langle T(d_{\boldsymbol{k},\sigma}(\tau)d^\dagger_{\boldsymbol{k},\sigma}(0))\rangle$, $\mathit{\Gamma}_\sigma(\boldsymbol{k},\tau) = -\langle T(d^\dagger_{-\boldsymbol{k},-\sigma}(\tau)d^\dagger_{\boldsymbol{k},\sigma(0)})\rangle$, $G'_\sigma(\boldsymbol{k},\tau) = -\langle T(d_{\boldsymbol{k}+\boldsymbol{Q},\sigma}(\tau)d^\dagger_{\boldsymbol{k},\sigma}(0))\rangle$, and $\mathit{\Gamma}'_\sigma(\boldsymbol{k},\tau) = -\langle T(d^\dagger_{-\boldsymbol{k}-\boldsymbol{Q},-\sigma}(\tau)d^\dagger_{\boldsymbol{k},\sigma}(0))\rangle$. Here T is the time-ordering operator which arranges other operators from right to left in the ascending order of imaginary time τ.

The first step of our scheme involves the calculation of imaginary time evolution of the operators $d_{\boldsymbol{k},\sigma}(\tau)$. As the next step, using the evolution, we obtain the equations of motion of the averages. The final step is the calculation of the Fourier coefficients of these temperature Green functions. The poles of the Fourier coefficients yields the single particle excitation spectra $E_{\boldsymbol{k}}(T < T_{\rm c})$. We find that $E_{\boldsymbol{k}}(T < T_{\rm c}) = \pm E^{(U,L)}(\boldsymbol{k})$, where $E^{(U,L)2}_{\boldsymbol{k}} = \left(\frac{1}{2}\right)[(\xi^2_{\boldsymbol{k}} + \xi^2_{\boldsymbol{k}+\boldsymbol{Q}} + 2D_{\rm eff}(\boldsymbol{k})^2) \pm p(\boldsymbol{k})]$, $\xi_{\boldsymbol{k}} = \varepsilon_{\boldsymbol{k}} - \mu$, $D^2_{\rm eff}(\boldsymbol{k}) = (\Delta^2_{\boldsymbol{k}} + \Delta^{(\rm SC)2}_{\boldsymbol{k}})$ and $p(\boldsymbol{k}) = [(\xi^2_{\boldsymbol{k}} - \xi^2_{\boldsymbol{k}+\boldsymbol{Q}})^2 + 4\Delta^2_{\boldsymbol{k}}(\xi_{\boldsymbol{k}} + \xi_{\boldsymbol{k}+\boldsymbol{Q}})^2]^{1/2}$. The quasi-particle excitations in cuprates, thus, have two gaps in the spectrum that are distinct and do not merge strictly into one "quadrature" gap $(D_{\rm eff}(\boldsymbol{k})^2 = [\Delta^2_{\boldsymbol{k}} + \Delta^{(\rm SC)2}_{\boldsymbol{k}}])$ if the *nesting property*, $\varepsilon_{\boldsymbol{k}} = -\varepsilon_{\boldsymbol{k}+\boldsymbol{Q}}$, of the dispersion is absent. For the near-nested situation we do obtain such a merger yielding $E_{\boldsymbol{k}} \approx [\xi^2_{\boldsymbol{k}} + D_{\rm eff}(\boldsymbol{k})^2]^{1/2}$. The two gaps in the excitation spectrum are then determined by the $1 \approx U_1 \sum_{\boldsymbol{k}}[(\cos k_x a - \cos k_y a)^2 \times \{\xi^2_{\boldsymbol{k}} + (\Delta^{(\rm PG)}_0(0)^2 + \Delta^{(\rm SC)}_0(0)^2)(\cos k_x a - \cos k_y a)^2\}^{-1/2}]$ and

$\Delta_k^{(\mathrm{SC})} \approx -(1/2)\sum_{\boldsymbol{k}',\sigma} V(\boldsymbol{k},\boldsymbol{k}')\Delta_{\boldsymbol{k}'}^{(\mathrm{SC})}/\sqrt{\xi_{\boldsymbol{k}'}^2 + D_{\mathrm{eff}}(\boldsymbol{k}')^2}$. The latter one is similar to the weak couplingBCS gap equation in the zero-temperature limit. Together with the equation to determine μ applying Luttinger theorem [8], the equations have been solved simultaneously. For the doping level 9.94% and temperatures $T = 60$ K and 20 K, for instance, we have found ($\mu/t_1 = -0.0018$, $\Delta_0^{(\mathrm{PG})}/t_1 = 0.0240$, $\Delta_0^{(\mathrm{SC})}/t_1 = 0.0150$), and ($\mu/t_1 = -0.0009$, $\Delta_0^{(\mathrm{PG})}/t_1 = 0.0170$, $\Delta_0^{(\mathrm{SC})}/t_1 = 0.0294$), respectively, for $((t_2/t_1) \approx 0.4$, $(t_3/t_1) = 0.0005)$. For the doping level 11.92% and temperatures $T = 85.9$ K, however, we have found ($\mu/t_1 = -0.0054$, $\Delta_0^{(\mathrm{PG})}/t_1 = 0.0044$, $\Delta_0^{(\mathrm{SC})}/t_1 = 0.0032$), for $((t_2/t_1) = 0.3925$, $(t_3/t_1) = 0.0005)$.

The exercise above leads to the graphical representations of $\pm E^{(U,L)}(\boldsymbol{k})$ in the co-existent DDW and DSC states. Before that, in Fig. 3 we have shown the contour plots of the momentum dependent carrier density in PG+SC state at 9.94% and 11.92% doping levels in the first Brillouin zone. In Fig. 2a we have shown the plot of single-particle excitation spectrum in the pure DDW phase (for the reference purpose) while in 3b–d the plots of $\pm E^{(U,L)}(\boldsymbol{k})$, along the antinodal cut $(-\pi,\pi)$–$(0,\pi)$–(π,π). In Fig. 2a, we find easy-to-notice PHA, as the upper band is parabolic while the lower band is characterized by dip at $(0,\ \pi)$, and the so-called back-bending momentum at $(-0.45,\pi)$ and $(0.45,\ \pi)$. In Fig. 2b–d, the bands $(-E_k^{(U,L)})$ below the Fermi energy are the reflected ones of those $(E_k^{(U,L)})$ above the Fermi energy. The shoulder-type feature of the dispersion $-E_k^{(L)}$, indicated by double-headed arrows, also exists in the experimental data [9]. The interplay of DDW and DSC is manifested by the fact that the band $(-E_k^{(L)})$ no more peak at $k_{\mathrm{F}}(0,\pi)$ but rather at the back-bending momentum position as shown in Fig. 2b–d. We conclude that the Bogoliubov quasi-particle band features observed in the superconducting state here are consistent with the ARPES experiments [9, 10].

References

[1] A. Levchenko, M.R. Norman, A.A. Varlamov, *Phys. Rev. B* **83**, 020506(R) (2011).

[2] A. Kanigel, U. Chatterjee, M. Randeria, M.R. Norman, G. Koren, K. Kadowaki, J.C. Campuzano, *Phys. Rev. Lett.* **101**, 137002 (2008).

[3] S. Hüfner, M.A. Hossain, A. Damascelli, G.A. Sawastzky, *Rep. Prog. Phys.* **71**, 062501 (2008).

[4] S. Chakravarty, R.B. Laughlin, D.K. Morr, C. Nayak, *Phys. Rev. B* **63**, 94503 (2001); I. Dimov, P. Goswami, Xun Jia, S. Chakravarty, *Phys. Rev. B* **78**, 134529 (2008); S. Chakravarty, *Rep. Prog. Phys.* **74**, 022501 (2011).

[5] K.A. Gschneidner, *Handbook on the Physics and Chemistry of Rare Earths*, Vol. 34, Elsevier, Amsterdam 2005, p. 165.

[6] K. Tanaka, T. Yoshida, A. Fujimori, D.H. Lu, Z.-X. Shen, X.-J. Zhou, H. Eisaki, Z. Hussain, S. Uchida, Y. Aiura, K. Ono, T. Sugaya, T. Mizuno, I. Terasaki, *Phys. Rev. B* **70**, 092503 (2004).

[7] The optimal doping $p_0 \approx 16\%$ is defined as the doping concentration with the highest superconducting transition temperature $T_{\mathrm{c}}(p_0)$. The doping beyond the optimal level yields normal metals with the Fermi liquid behavior and with decreasing T_{c}. The underdoped cuprate superconductors are characterized by the fact that T_{c} increases when doping is increased with respect to optimal doping; the pseudo-gap temperature T^* is close to T_{c} near optimal doping. The temperature T^* decreases with the increasing doping.

[8] J.M. Luttinger, *Phys. Rev.* **119**, 1153 (1960); M.M. Korshunov, S.G. Ovchinnikov, *Phys. Solid State* **45**, 1415 (2003).

[9] M. Hashimoto, Rui-Hua He, K. Tanaka, J.P. Testaud, W. Meevasana, R.G. Moore, Donghui Lu, Hong Yao, Y. Yoshida, H. Eisaki, T.P. Devereaux, Z. Hussain, Z.-X. Shen, *Nature Phys.* **6**, 414 (2010).

[10] H.-B. Yang, J.D. Rameau, P.D. Johnson, T. Valla, A. Tsvelik, G.D. Gu, *Nature* **456**, 77 (2008).